THE JOURNAL OF BIOLOGICAL CHEMISTRY VOL. 287, NO. 51, pp. 43170–43179, December 14, 2012

A Single Residue within the V5 Region of HIV-1 Envelope Facilitates Viral Escape from the Broadly Neutralizing Monoclonal Antibody VRC01*

Received for publication, July 9, 2012, and in revised form, October 23, 2012 Published, JBC Papers in Press, October 25, 2012, DOI 10.1074/jbc.M112.399402

Dongxing Guo[‡], Xuanling Shi[§], Kelly C. Arledge[§], Dingka Song[§], Liwei Jiang[§], Lili Fu[§], Xinqi Gong[¶], Senyan Zhang[¶], Xinquan Wang[¶], and Linqi Zhang[‡§1]

From the [‡]AIDS Research Center, MOH Key Laboratory of Systems Biology of Pathogens, Institute of Pathogen Biology, Chinese Academy of Medical Sciences and Peking Union Medical College, Beijing 100730 and the [§]Comprehensive AIDS Research Center and Research Center for Public Health, School of Medicine, and the [¶]Center for Structural Biology, School of Life Sciences, Tsinghua University, Beijing 100084, China

Background: We aim to define the critical residues on the surface glycoprotein of HIV-1 responsible for VRC01 resistance.
Results: We found that a single asparagine residue, a potential *N*-linked glycosylation site, within the V5 region is associated with VRC01 resistance in the viral strains studied.
Conclusion: The V5 region is the major determinant of VRC01 resistance.
Significance: This work will help to us to better understand interplay between HIV-1 and VRC01.

VRC01, a broadly neutralizing monoclonal antibody, is capable of neutralizing a diverse array of HIV-1 isolates by mimicking CD4 binding with the envelope glycoprotein gp120. Nonetheless, resistant strains have been identified. Here, we examined two genetically related and two unrelated envelope clones, derived from CRF08_BC-infected patients, with distinct VRC01 neutralization profiles. A total of 22 chimeric envelope clones was generated by interchanging the loop D and/or V5 regions between the original envelopes or by single alanine substitutions within each region. Analysis of pseudoviruses built from these mutant envelopes showed that interchanging the V5 region between the genetically related or unrelated clones completely swapped their VRC01 sensitivity profiles. Mutagenesis analysis revealed that the asparagine residue at position 460 (Asn-460), a potential *N*-linked glycosylation site in the V5 region, is a key factor for observed resistance in these strains, which is further supported by our structural modeling. Moreover, changes in resistance were found to positively correlate with deviations in VRC01 binding affinity. Overall, our study indicates that Asn-460 in the V5 region is a critical determinant of sensitivity to VRC01 specifically in these viral strains. The long side chain of Asn-460, and potential glycosylation, may create steric hindrance that lowers binding affinity, thereby increasing resistance to VRC01 neutralization.

HIV-1 mediates cell entry through the trimeric envelope glycoprotein gp160, which is in turn composed of exterior receptor-binding gp120 subunits and the fusion-mediating transmembrane gp41 regions (1–4). Entry is a multistep process, initiated by gp120 binding with the target cell receptor, CD4 (5, 6), which triggers the extensive conformational changes that facilitate binding with either the CCR5 or CXCR4 co-receptor, and the subsequent series of events that lead to fusion with the target cell membrane (7–11). The CD4-binding site (CD4bs)[2] on gp120 is critical for viral entry and highly conserved compared with other envelope contact regions. The CD4bs is also the viral Achilles heel, containing the key epitopes and domains recognized by broadly neutralizing monoclonal antibodies (bnmAb) and polyclonal sera from "elite neutralizers," individuals with exceptionally strong immune control over viral replication (12–16). Better understanding of the intricate interplay between the CD4bs and antibody neutralization will provide critical insights into HIV-1 pathogenesis and aid the development of effective CD4bs-directed vaccines and therapeutics.

In recent years, tremendous progress has been made in the isolation and characterization of bnmAbs from elite neutralizers that target the CD4bs on gp120 (12–17). The first such bnmAb, b12, was isolated from a phage display library and is capable of neutralizing about 35% of a large multiclade panel of pseudotyped viruses (17, 18). The second, HJ16, was isolated through *in vitro* immortalization of memory B cells from a clade C-infected patient, and it demonstrated similar breadth to that of b12 (19). With recent advancements in micro-culturing and antigen-specific sorting of B cells from elite neutralizers, researchers have isolated increasing numbers of bnmAbs directed to the CD4bs, including VRC01, VRC03, 3BNC117, 3BNC55, VRC-PG04, and NIH45–46 (12–17, 20). Many in this new generation of bnmAbs have demonstrated significantly higher potency and breadth compared with b12 and HJ16. The prototype VRC01, for instance, was isolated from a clade B-infected individual and neutralized 91% of a diverse panel of pseu-

* This work was supported by National Science and Technology Major Projects 2012ZX10001-006 and 2012ZX10001-009, National Outstanding Youth Award 30825035, National Natural Science Funds U0832604 and 81101236, the Tsinghua University Initiative Scientific Research Program, and the Tsinghua Yue-Yuen Medical Sciences Fund.

[1] To whom correspondence should be addressed: Comprehensive AIDS Research Center, School of Medicine, Tsinghua University, Beijing, 100084, China. Tel.: 86-10-6278–8131; Fax: 86-10-6279-7732; E-mail: zhanglinqi@tsinghua.edu.cn.

[2] The abbreviations used are: CD4bs, CD4-binding site; bnmAb, broadly neutralizing monoclonal antibody; PNGS, potential *N*-linked glycosylation site.

dotyped viruses (13). VRC03, a close relative of VRC01, was able to neutralize about 57% of these (13). More recently isolated CD4bs-directed bnmAbs, in particular 3BNC117, 3BNC55, VRC-PG04, and NIH45–46, have shown similar or even higher potency and breadth compared with prototype VRC01 (14–16). Most of these VRC01-like bnmAbs show convergence on their recognition to the CD4-binding site on the gp120, even though some of them induce conformational changes on soluble gp120. Their primary mechanism of neutralization should be blocking the interaction between the virus and receptor CD4 as they compete for the same general area on HIV-1 gp120, although it is worth noting that there may be differences in their mechanisms of blocking the gp120-CD4 receptor interaction (12–17, 19–24).

Unfortunately, despite the superior potency and breadth of these bnmAbs, each fails to neutralize a small, but significant, portion of pseudotyped virus panels. VRC01, for instance, is unable to neutralize about 10% of tested viruses (13), and many of those resistant strains were not derived from elite neutralizers like the donor from which VRC01 was initially isolated. The rise of VRC01-resistant viruses in these "ordinary" individuals suggests that such variants are either naturally occurring or selected under a VRC01-like antibody response at some point during disease progression. VRC01-resistant strains have also been identified in the VRC01 donor (25). Only selective archival proviral Env variants remained sensitive, whereas all contemporary plasma-derived variants are resistant, indicating a rapid genetic and phenotypic evolution under the strong antibody-based selection pressure (25). Collectively, these results indicate that viruses resistant to VRC01, and anti-CD4bs mAbs as a whole, are consistently being generated with or without the unique immune selection pressures found in "elite controllers," imposing tremendous challenge for preventative and therapeutic interventions based on these bnmAbs.

The mechanism of viral resistance to VRC01 is perhaps the best studied among all these anti-CD4bs bnmAbs. Structural analysis of VRC01 bound to monomeric gp120 shows it binds to the CD4bs, although it makes less contact with the variable inner domain and the β20–β21 segment of the bridging sheet compared with the mAb b12 (26). Instead, there is greater contact with loop D, the base of the V5 loop region, and β24. These segments are essential contact regions for VRC01 with the envelope spike and likely play a key role in viral escape. Analysis of viruses displaying natural resistance to VRC01 and mutagenesis studies of clade B viruses have suggested mutations in either the loop D and V5 regions or a combination of both may be critical for natural evasion of VRC01 (27). However, the resistance mechanisms of non-clade B viruses are currently unknown. In the course of characterizing diverse HIV-1 strains isolated from infected patients in China, we identified two genetically related and two unrelated envelope clones, derived from CRF08_BC-infected patients, with distinct VRC01 neutralization profiles (28). Here, we show that interchanging the V5 region between clones within both sets completely swapped their VRC01 sensitivity profiles. Mutagenesis analysis revealed that the asparagine residue at position 460 (Asn-460), a potential *N*-linked glycosylation site (PNGS) in the V5 region, plays a critical role in determining viral sensitivity of these strains to VRC01, whereas other residue changes seemed to have no discernible impact. Structural modeling indicates there is a potential clash between the long side chain at position Asn-460 and the arginine residue at position 61 (Arg-61) on the heavy chain of VRC01. We propose that such steric hindrance from the Asn-460 side chain, potentially enhanced by *N*-linked glycosylation, would lower binding affinity with and thereby increase resistance to VRC01 neutralization.

EXPERIMENTAL PROCEDURES

CRF08_B′C Envelope Clones and CRF_08B′C Plasma Pool—Two genetically related full-length envelope molecular clones, CNE47 and CNE48, were isolated from the peripheral blood mononuclear cell of an HIV-1 CRF08_B′C-infected intravenous drug user as reported previously (28). This patient had received highly active antiretroviral therapy (HAART) for 5 years, and plasma viral loads were well suppressed (<50 copies/ml), with peripheral blood CD4 T cell levels >350 cells/μl. Two genetically unrelated full-length envelope clones, CNE23 and CNE30, were isolated from two separate CRF08_B′C-infected intravenous drug users who had never been on antiretroviral therapy at the time of sampling (28).

Genomic DNA was extracted according to QIAamp DNA blood mini kit protocols (Qiagen, Shanghai, China). Full-length envelope sequences were amplified by nested PCR with HIV-1 subtype B′C-specific primers as reported previously (20). The PCR product was cloned into pcDNA 3.1 expression vectors (Invitrogen) and then verified by sequencing. The full-length gp160 amino acid sequences were analyzed based on comparison with HIV-1 HXB2.

The HIV-1 CRF08_B′C plasma pool was generated by mixing equal portions of plasma samples from HIV-1 CRF08_B′C-infected patients as described previously (28). All plasma samples were heat-inactivated for 1 h at 56 °C and stored at −80 °C until use. None of the patients from which the plasma pool was derived had ever been on antiretroviral therapy at the time of sampling. The plasma and peripheral blood mononuclear cell samples were obtained from HIV-1-infected individuals with informed consent. This study was approved by the ethic committees at the appropriate institutions (28).

Antibodies and Soluble CD4 (sCD4)—The IgG-1 VRC01 antibodies were kindly provided by Dr. John Mascola (Vaccine Research Center, NIAID, National Institutes of Health). Samples of IgG-1 b12 were obtained from the AIDS Research and Reagents Program (National Institutes of Health). The IgG-4 ibalizumab was kindly provided by Dr. David D. Ho (Aaron Diamond AIDS Research Center, The Rockefeller University). Soluble CD4 (sCD4) protein was produced by Progenics Pharmaceuticals, Inc (Tarrytown, NY).

Generation of Chimeric Clones and Site-directed Mutagenesis—The CNE47/CNE48 and CNE23/CNE30 chimeric clones were constructed based on the original full-length gp160 sequences published previously (28). The single alanine substitutions were performed using pcDNA 3.1 expression vectors according to the protocols in QuikChange XL site-directed Mutagenesis kit (Invitrogen). All mutant clones were confirmed by sequencing.

Pseudovirus Production—The HIV-1 *env*-pseudovirus were generated as described previously (28). Briefly, pcDNA 3.1

expression vectors containing target *env* genes were co-transfected with a pNL4–3R-E-luciferase viral backbone plasmid into 293T cells at a 1:3 ratio. The cell culture medium was replaced with 10% FBS/DMEM after 4–6 h and then incubated for an additional 40–48 h at 37 °C. Pseudoviral supernatants were collected after 48 h. Viral titers were then quantified as a measure of luciferase activity in relative light units (Bright-Glo Luciferase Assay System, Promega Biosciences). Supernatants were packaged and stored at −80 °C.

Analysis of Viral Sensitivity to Neutralization—Neutralization assays were performed by incubating 100 $TCID_{50}$ of each pseudovirus with either VRC01, b12, soluble CD4, or pooled B′C subtype plasma for 1 h at 37 °C. Neutralizing samples were added in eight serial 1:3 dilutions from either an initial concentration of 50 μg/ml for purified proteins or an initial dilution of 1:20 for pooled plasma. Each assay was then incubated with TZM-bl cells ($\sim 1.5 \times 10^4$/well). Infectivity was quantified as a measure of luciferase activity (relative light units) 48 h post-infection. Half-maximal inhibitory concentrations (IC_{50}) were reported as the concentration required to inhibit infection by 50% compared with the controls. The IC_{50} values were calculated using the dose-response inhibition model with a variable slope in GraphPad Prism, version 5.0 (GraphPad Software Inc., La Jolla, CA).

Analysis of Envelope Binding to VRC01, b12, sCD4, and HIV-1 B′C Pooled Plasma—Binding affinities of CNE47, CNE48, CNE23, CNE30, and chimeric pseudoviruses to either monoclonal antibody or soluble CD4 were measured by a gp120-capture enzyme-linked immunosorbent assay. Monomeric gp120 was obtained by incubating pseudoviral supernatants with 0.5% Triton X-100 for 5 min at room temperature. A 96-well plate was coated overnight at 4 °C with D7324, an anti-gp120 sheep C5 antibody, and then each well was incubated with 100 μl of a monomeric gp120, 0.5% Triton mix for 1 h and washed three times with PBST. Wells were blocked for 2 h at 37 °C with 1% bovine serum albumin in PBS. Secondary antibodies VRC01 or b12, sCD4, and the HIV-1 B′C plasma pool were incubated for 1 h at 37 °C. Each mAb was added in eight serial 1:3 dilutions from 50 μg/ml and the plasma pool in eight serial 3-fold dilutions from an initial 1:500 concentration (100 μl/well). Washes and incubation times were repeated. Horseradish peroxidase-conjugated anti-human Ig (Abcam Ltd., Hong Kong) were used, as appropriate, for immunodetection. Maximum binding concentrations were recorded at peak absorbencies of 450 nm. The 50% effective concentrations (EC_{50}) were calculated using the sigmoidal dose-response model with a variable slope in GraphPad Prism, version 5.0 (GraphPad Software Inc., La Jolla, CA). The B′C plasma pool was used as a base-line quantification of monomeric gp120.

Structural Modeling and Analysis—Structural modeling of gp120 with different V5 regions in complex with VRC01 was conducted as described previously (28). Briefly, the gp120 structure (clade A/E 93TH057) from the complex with antibody VRC01 (Protein Data Bank code 3NGB) was used as a template, and the V5 region was replaced by the sequences from either CNE 47 or CNE48. The loop modeling protocol in Rosetta 3.3 was used for the two loops, from Arg-456 to Phe-468 in CNE47 and from Arg-456 to Phe-468 in CNE48 (29). In this protocol, the torsion angles (ϕ/ψ) and N–CA–C bond angles were optimized using the simulated annealing Metropolis Monte Carlo algorithm. Two separate ensembles of 10 models were built for CNE47 and CNE48. They were then docked onto VRC01 with 3NGB as the template. Figures of structural interactions were made with the program PyMOL (DeLano Scientific, San Carlos, CA).

Statistical Analysis—Relationships between neutralization sensitivity to and binding affinity with either VRC01 or sCD4 proteins were analyzed by SPSS software, version 16.0. The Mann-Whitney *U* test was used to compare the differences in median values between different groups.

RESULTS

Isolation of CRF08_B′C Envelope Clones from an Infected Individual with Distinct Neutralization and Binding Profiles to VRC01—Our laboratory recently characterized the neutralization sensitivities of HIV-1 *Env* clones isolated from chronically infected patients in China (28). Among them, we identified two CRF08_B′C *Env* clones (CNE47 and CNE48), isolated at a single time point from the same individual, which displayed substantial differences in their sensitivities to VRC01 neutralization. Protein sequence alignments revealed the two clones were over 94% identical, with polymorphic amino acid and length differences scattered throughout (Fig. 1*A*). Focusing our analyses on the key VRC01 contact regions, no variations were found in the CD4-binding loop and only a single residue difference was observed in the loop D region at position A281V, which has previously been shown not to interact wth VRC01 binding (27). However, CNE47 contained four distinct residues in the V5 region, of which three (asparagine-glutamic acid-threonine) were insertions that generated an additional PNGS at position 460 in the V5 region (Fig. 1*A*). Pseudoviruses built from these two envelope proteins showed that CNE47 was more resistant (IC_{50} = 9.27 μg/ml) to VRC01 relative to CNE48 (IC_{50} = 0.39 μg/ml) (Fig. 1*B*, and Table 1). In binding assays, CNE47 also demonstrated a weaker affinity for VRC01, with an EC_{50} of about 12.21 μg/ml compared with 2.40 μg/ml for CNE48. In addition, we found that mutational differences between the clones did not affect their interactions with sCD4, b12, or the plasma pool derived from HIV-1 subtype B′C-infected patients (Fig. 1*B* and Table 1). Both clones are naturally resistant to b12 and, on a range of all isolates derived from infected patients in China, have medium level sensitivities to sCD4 and plasma pools neutralization (Fig. 1*B*). Based on these results, we aimed to determine whether the mutations facilitating viral escape of CNE47 from VRC01 could be narrowed down to the V5 region, a particular residue, or residues within.

V5 Region Determines Viral Sensitivity to VRC01 Neutralization and Binding—We constructed a total of eight chimeric Env pseudoviruses, altering wild-type CNE47 and CNE48 sequences by exchanging either the loop D, the V5 region, the V5/β24 region, or the loop D/V5/β24 regions combined between the two clones (Table 1). As shown in Table 1 and Fig. 2*A*, chimeric CNE47 pseudoviruses containing the V5 region from CNE48 (clones 3–5) were significantly more sensitive to VRC01 neutralization (0.55–1.08 μg/ml), similar to wild-type CNE48 (0.39 μg/ml). Conversely, for CNE48 pseudoviruses,

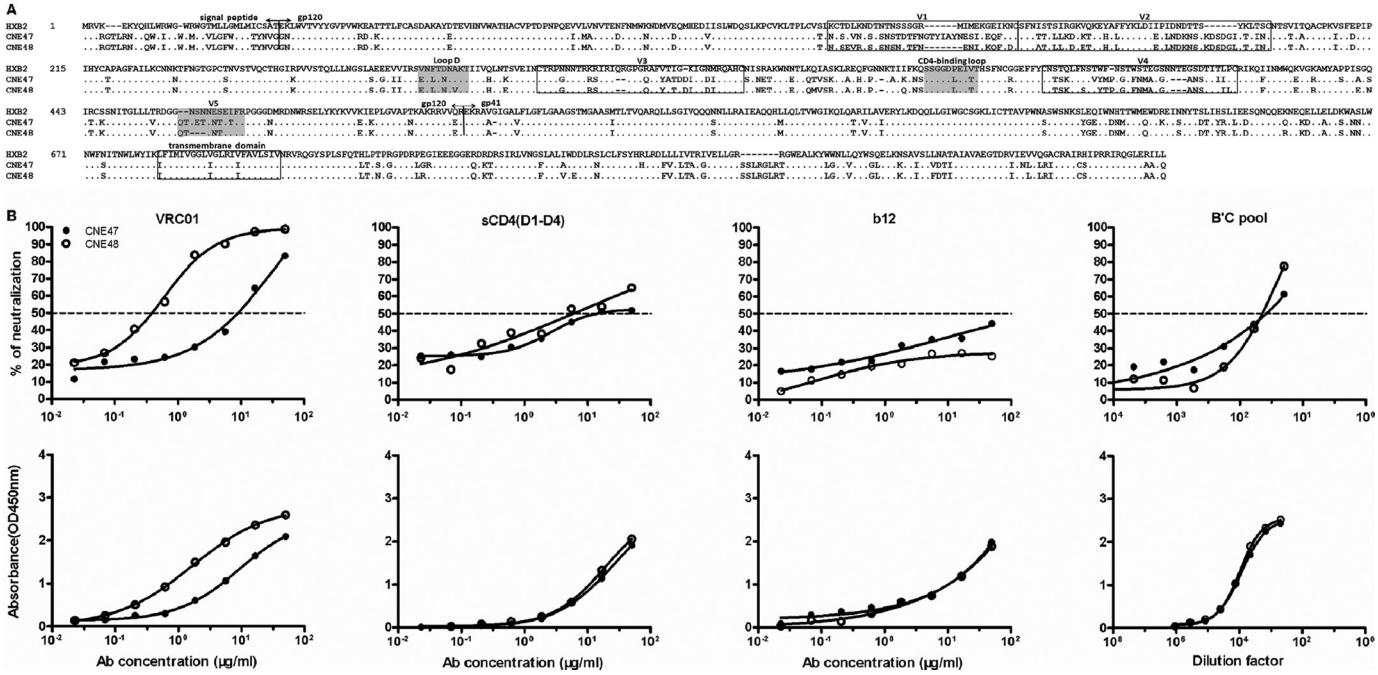

FIGURE 1. **Genotypic and phenotypic comparison between CNE47 and CNE48.** The gp160 amino acid sequences of CNE47 and CNE48 are shown aligned against the HXB2 reference strain. Regions known to interact with VRC01, including the CD4-binding loop, loop D, and V5 regions, are *highlighted*. Hypervariable regions *V1, V2, V3, V4, V5,* and the *trans-membrane domain* are *boxed* (*A*). Pseudoviruses expressing full-length Env from either CNE47 or CNE48 were assayed for neutralization sensitivity and binding affinity with VRC01, sCD4, b12, and HIV-1 B′C plasma pool (*B*). CNE47 pseudoviruses (*solid circle*) were distinctly more resistant (IC_{50} = 9.27 μg/ml) to VRC01 relative to CNE48 pseudoviruses (*open circle*) (IC_{50} = 0.39 μg/ml). ELISA results showed CNE47 gp160 had a much weaker binding affinity for VRC01 (EC_{50} of 12.21 μg/ml) compared with that of CNE48 (EC_{50} of 2.40 μg/ml). No measurable differences were found between the wild-type Env pseudoviruses in terms of their sCD4, b12, or B′C plasma pool neutralization and binding profiles.

TABLE 1

Neutralization and binding profiles of mutant viruses for VRC01, b12, ibalizumab, and sCD4

Chimeric pseudoviruses containing loop D and/or V5 regions from the VRC01-resistant CNE47 or CNE23 are italics. Variations from the reference β24 region and single alanine substitutions in the V5 region are underlined. The neutralization and binding activity of mutant viruses to VRC01, b12, ibalizumab, and sCD4 are shown, along with comparisons as a percent of their respective wild-type activity. The gp160 sequences of wild-type CNE47, CNE48, CNE23, and CNE30 are referenced against HIV-1 HXB2 to map the loop D (residues 276–283) and V5/β24 regions (residues 458–469).

Clone number	Virus	Env sequence			Neutralization activities								Binding affinity			
		loop D	V5/β24		VRC01		b12		Ibalizumab		sCD4 (D1-D4)		VRC01		sCD4 (D1-D4)	
		(276-283)	(458-469)		IC_{50} (μg/ml)	% of WT	IC_{50} (μg/ml)	% of WT	IC_{50} (μg/ml)	% of WT	IC_{50} (μg/ml)	% of WT	EC_{50} (μg/ml)	% of WT	EC_{50} (μg/ml)	% of WT
1	CNE47	NLTNNAKT	GGQT*NETNNTE*	TFR	9.27	100	>50	100	0.17	100	16.98	100	12.21	100	10.26	100
2	CNE47-D-48	NLTNNVKT	GGQT*NETNNTE*	TFR	9.27	100	>50	100	0.12	70.59	10.72	63.10	18.90	154.88	10.26	100
3	CNE47-V5-48	NLTNNAKT	GGQT---NNTE	TFR	1.08	11.65	>50	100	0.05	29.41	>50	>294	5.49	44.96	20.81	202.77
4	CNE47-V5/β24-48	NLTNNAKT	GGQT---NNTE	IFR	0.55	5.93	>50	100	0.10	58.82	>50	>294	3.92	32.13	10.26	100
5	CNE47-D/V5/β24-48	NLTNNAKT	GGQT---NNTE	IFR	0.87	9.39	>50	100	0.12	70.59	>50	>294	4.86	39.80	13.53	131.83
6	CNE47-N460A	NLTNNAKT	GGQT*A*ETNNTE	TFR	1.61	17.37	>50	100	0.10	58.82	>50	>294	12.21	100	8.15	79.43
7	CNE47-E461A	NLTNNAKT	GGQT*NA*TNNTE	TFR	9.27	100	>50	100	0.17	100	>50	>294	8.31	68.05	10.26	100
8	CNE47-T462A	NLTNNAKT	GGQT*NEA*NNTE	TFR	14.79	159.55	>50	100	0.08	47.06	>50	>294	8.31	68.05	8.15	79.43
9	CNE47-N463A	NLTNNAKT	GGQT*NETA*NTE	TFR	6.21	66.99	>50	100	0.17	100	>50	>294	12.21	100	8.15	79.43
10	CNE47-N460/463A	NLTNNAKT	GGQT*A*ET*A*NTE	TFR	1.26	13.59	>50	100	0.35	206	22.39	131.86	7.08	57.99	10.20	99.42
11	CNE48	NLTNNVKT	GGQT---NNTE	IFR	0.39	100	>50	100	0.13	100	5.85	100	2.40	100	9.04	100
12	CNE48-D-47	NLTNNAKT	GGQT---NNTE	IFR	0.68	174.36	>50	100	0.07	53.85	1.38	23.60	1.56	65.07	5.70	63.10
13	CNE48-V5-47	NLTNNVKT	GGQT*NETNNTE*	IFR	28.18	7225.64	>50	100	0.29	223.08	2.88	49.30	7.02	292.66	5.70	63.10
14	CNE48-V5/β24-47	NLTNNVKT	GGQT*NETNNTE*	TFR	16.22	4158.97	>50	100	0.07	53.85	2.25	38.55	5.67	236.24	7.52	83.18
15	CNE48-D/V5/β24-47	NLTNNAKT	GGQT*NETNNTE*	TFR	10.72	2748.72	>50	100	0.05	38.46	4.86	83.18	8.64	360.05	8.24	91.20
16	CNE48-N463A	NLTNNVKT	GGQT---A*N*TE	IFR	0.87	223.08	>50	100	1.26	969.23	22.39	382.82	4.84	201.67	9.04	100
17	CNE23	NLT*D*NAKT	GGT-NLTAELNQTE	IFR	19.50	100	4.05	100	0.04	100	>50	100	2.40	100	10.34	100
18	CNE23-V5-30	NLT*D*NAKT	GGTTNNT---NNTE	IFR	0.62	3.18	5.01	123.70	0.08	200	>50	100	0.72	30.04	12.03	116.41
19	CNE23-N460A	NLT*D*NAKT	GGT-A*L*TAELNQTE	IFR	1.05	5.38	2.04	50.41	0.05	128	>50	100	0.79	33.10	10.34	100
20	CNE23-N463A	NLT*D*NAKT	GGT-NLTAELA*Q*TE	IFR	7.94	40.72	2.04	50.41	0.07	165	>50	100	2.51	104.66	10.34	100
21	CNE23-N460/463A	NLT*D*NAKT	GGT-A*L*TAELA*Q*TE	IFR	0.23	1.19	1.41	34.88	0.13	321	>50	100	0.79	33.10	10.34	100
22	CNE30	NLTNNAKT	GGTTNNT---NNTE	IFR	0.72	100	6.41	100	0.09	100	1.56	100	2.80	100	15.00	100
23	CNE30-V5-23	NLTNNAKT	GGT-NLTAELNQTE	IFR	5.01	695.83	7.03	109.65	0.24	266.67	16.22	1039.92	4.80	171.43	18.04	120.23
24	CNE30-N460A	NLTNNAKT	GGTT*A*NT---NNTE	IFR	0.32	43.89	6.41	100.00	0.16	176.10	50.01	3205.77	3.31	118.26	15.00	100
25	CNE30-N463A	NLTNNAKT	GGTTNNT---A*N*TE	IFR	0.26	36.53	2.45	38.29	0.11	126.99	28.84	1848.74	3.89	138.94	15.00	100
26	CNE30-N460/463A	NLTNNAKT	GGTT*A*NT---A*N*TE	IFR	0.08	10.97	1.87	29.17	0.79	882.59	28.84	1848.74	3.89	138.94	15.00	100

inserting the CNE47 V5 region either alone (clone 13), with V5/β24 (clone 14), or together with loop D (clone 15) increased VRC01 resistance to a degree comparable with that of wild-type CNE47 (Table 1 and Fig. 2*A*). Within each group of chimeric pseudoviruses, we found the degree of change was the same regardless of whether V5 was exchanged alone or in combination with β24 and the loop D region (Table 1 and Fig. 2*A*). As expected, exchanging only the loop D region between CNE47

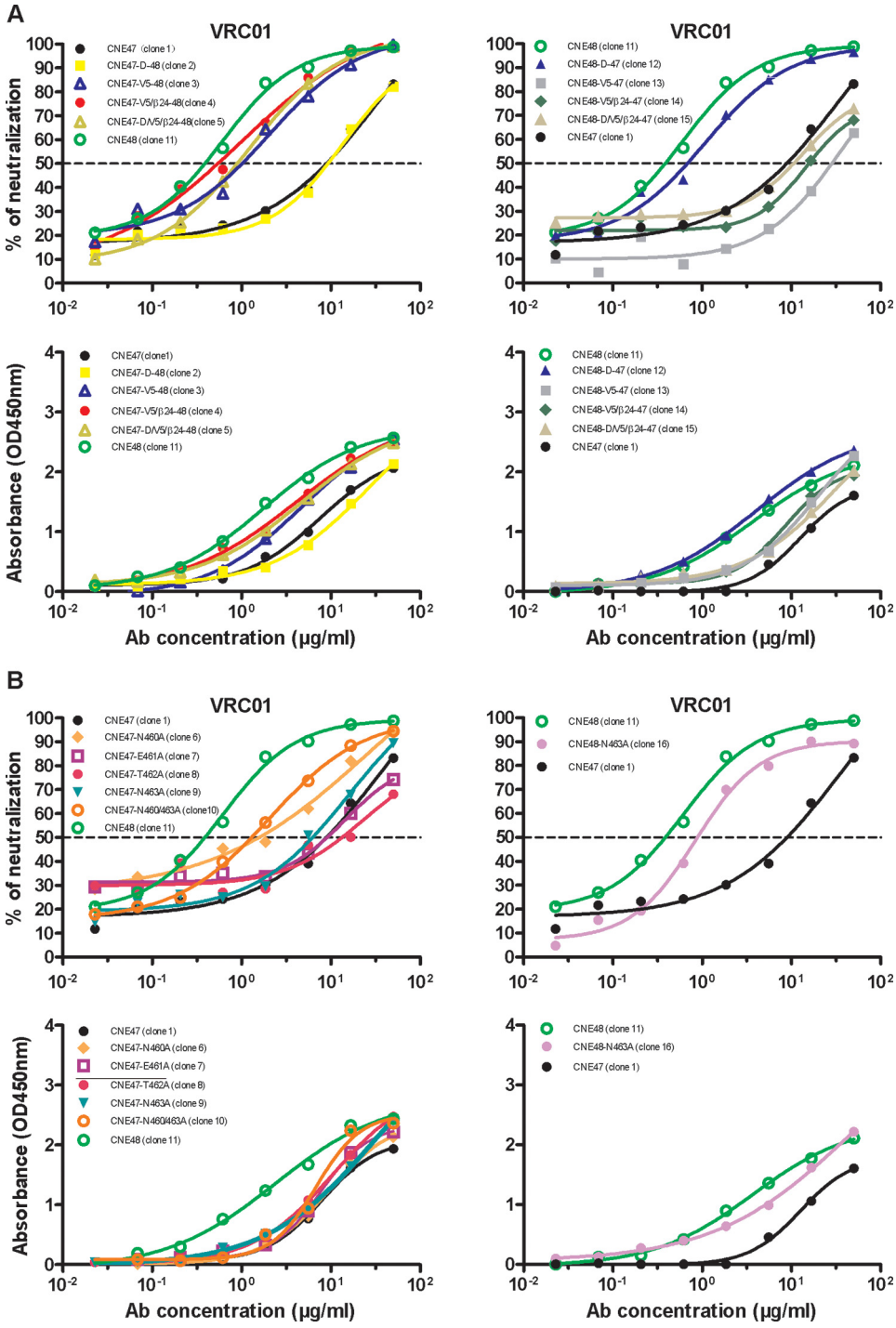

FIGURE 2. **Comparisons of mutant viruses containing either swapped regions (*A*) or single alanine substitutions (*B*) in terms of neutralization sensitivity to or binding affinity with VRC01.** Mutant CNE47 viruses containing the CNE48 V5 region (clones 3–5) became more sensitive to VRC01, although swapping only the loop D region (clone 2) did not measurably affect sensitivity. Conversely, mutant CNE48 viruses containing the CNE47 V5 region (clones 13–15) showed greater resistance to VRC01. Altering only the loop D region had a minimal effect on sensitivity (*A*, *upper panels*). Differences in ELISA binding profiles complemented the observed trend in neutralization sensitivities, although changes were not as pronounced (*A*, *lower panels*). Among CNE47 mutant viruses containing single alanine mutations, only CNE47-N460A (*orange*) showed significantly increased neutralization sensitivity to VRC01 relative to wild-type (*B*, *upper panels*). The CNE48 Env had only one PNGS, Asn-463, for analysis in the V5 region (CNE48-N463A), and mutation here did not alter neutralization sensitivity (*B*, *upper panel*). Again, trends across ELISA binding profiles reflected those for neutralization sensitivity, with changes less pronounced (*B*, *lower panels*).

(clone 2) and CNE48 (clone 12) did not alter resistance profiles (Table 1 and Fig. 2*A*) as both clones share almost identical sequence. In terms of binding affinity, although changes between chimeric pseudoviruses were not as pronounced as those measured for neutralization sensitivity, significant deviations from wild type were primarily detected when V5 regions were swapped (Fig. 2*A* and Table 1). Taken together, these results provide strong evidence that the V5 region is the key determinant of VRC01 neutralization sensitivity and binding affinity in these viral strains.

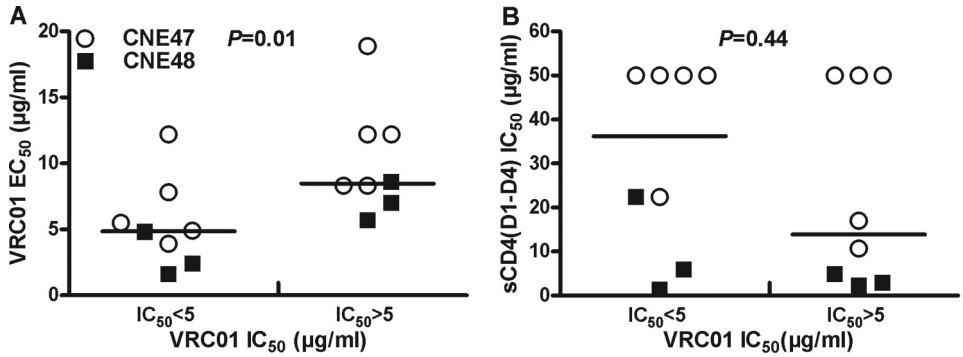

FIGURE 3. **Correlative analysis of VRC01 neutralization and binding.** Binding activities of monomeric gp120 derived from CNE47 and CNE48 pseudoviruses were compared between VRC01-sensitive ($IC_{50} < 5$ μg/ml) and VRC01-resistant ($IC_{50} > 5$ μg/ml) groups (*A*). Soluble CD4 (sCD4) neutralization sensitivities were compared across the same groups (*B*). The *horizontal lines* indicate mean EC_{50} or IC_{50} values. The Mann-Whitney test was used to derive *p* values, with a statistical significance of $p < 0.05$.

To further support this hypothesis, we studied two genetically unrelated CRF08_B′C envelope clones, CNE23 and CNE30, derived from separate individuals. When tested against VRC01 as pseudovirus constructs, CNE23 was significantly more resistant to neutralization (IC_{50} = 19.50 μg/ml) relative to CNE30 (IC_{50} = 0.72 μg/ml) (Table 1). Following the described methods, V5 regions were exchanged between clones and analyzed for changes in neutralization sensitivity. The chimeric clones showed a 30-fold decrease in IC_{50} values for CNE23 (clone 18) and a near 7-fold increase for CNE30 (clone 23), compared with their respective wild-types (Table 1). These results aligned with our initial findings and confirmed that the V5 region plays a key role in the interaction between VRC01 and the CRF08_B′C HIV-1 envelope glycoprotein.

Asparagine Residue at Position 460 (Asn-460) within the V5 Region Facilitates VRC01 Resistance—To investigate the relative contribution of individual residues within the Env protein to the VRC01 resistance, we generated a series of CNE47 and CNE48 pseudoviruses containing single alanine substitutions in the V5 region, and we analyzed for changes in binding and neutralization sensitivity compared with wild type. As shown in Table 1 and Fig. 2*B*, substitutions at positions 461, 462, and 463 in CNE47 (clones 7–9) did not significantly impact neutralization sensitivity. However, substituting asparagine for alanine at position 460 alone (clone 6) or in combination with Asn-463 (clone 10), substantially lowered the IC_{50} from 9.27 to 1.61 or 1.26 μg/ml, respectively (Table 1). Interestingly, although alanine substitution at position 462 would also preclude glycosylation at Asn-460, there was no change in the neutralization sensitivity of such a mutant (clone 8). This suggests that the asparagine residue itself, irrespective of glycosylation, confers VRC01 resistance. Furthermore, eliminating the other PNGS alone at position 463 (clones 9 and 16) did not measurably impact neutralization in either CNE47 or CNE48 mutants. Collectively, these results indicate that Asn-460 is the major determinant of observed resistance, and although glycosylation may enhance this effect, it is not necessarily required. The contributions of other residues within the V5 and loop D regions are either relatively small or barely detectable.

To further confirm the role of Asn-460 in VRC01 resistance in genetically unrelated strains, we generated a series of CNE23 and CNE30 pseudoviruses containing single alanine substitutions in the V5 region, and we analyzed for changes in binding and neutralization sensitivity compared with wild type. As shown in Table 1, substituting asparagine for alanine at position 460 alone (clone 19) or in combination with Asn-463 (clone 21) substantially lowered the IC_{50} for CNE23 from 19.50 to 1.05 or 0.23 μg/ml, respectively (Table 1). A moderate reduction in IC_{50} was found when substituting asparagines at position 463 (clone 20). Furthermore, despite being a sensitive strain to VRC01, alanine substitutions at 460 or 463 alone or in combination in CNE30 resulted in further increases to VRC01 neutralization (clones 24–26). These results are consistent with our initial findings and highlight the major role of Asn-460 in facilitating strain sensitivity to VRC01 neutralization, whereas that for Asn-463 is detectable but relatively minor.

Neutralization Sensitivity Is Determined by the Binding Affinity with VRC01—As shown above, greater VRC01 resistance corresponded with a weaker binding affinity in both wild-type and chimeric CNE47 and CNE48 clones. To test the strength of this correlation, we analyzed the binding affinity (EC_{50}) with VRC01 and sCD4 of recombinant Env clones illustrated above (Fig. 3). For each strain, wild-type, chimeric, and single mutant pseudoviruses were divided into two groups based on whether their observed VRC01 neutralization sensitivities fell above (resistant) or below (sensitive) an IC_{50} of 5 μg/ml, and then we evaluated the degree of association with their respective EC_{50} values. As expected, for both CNE47 and CNE48 pseudoviruses, binding affinity EC_{50} was significantly lower for the VRC01-sensitive group than for resistant pseudoviruses (Fig. 3*A*, $p = 0.01$), although a couple of outlier strains were also found. However, cross-analysis between sCD4 binding and VRC01 neutralization sensitivity failed to show any statistical association (Fig. 3*B*, $p = 0.44$).

Neutralization Sensitivity of Chimeric Pseudoviruses to b12, Ibalizumab, and sCD4—We also investigated whether genetic substitutions in the V5 regions affected neutralization sensitivities to reagents known to interfere with the gp120-CD4 receptor interaction, including sCD4, bnmAb b12, and ibalizumab, a nonimmunosuppressive monoclonal antibody that binds CD4 and has been shown to inhibit entry of diverse HIV-1 isolates. As displayed in Fig. 4 and Table 1, of the chimeric and alanine mutant pseudoviruses derived from either the CNE47/CNE48 group or the CNE23/CNE30 group, none had altered infectivity

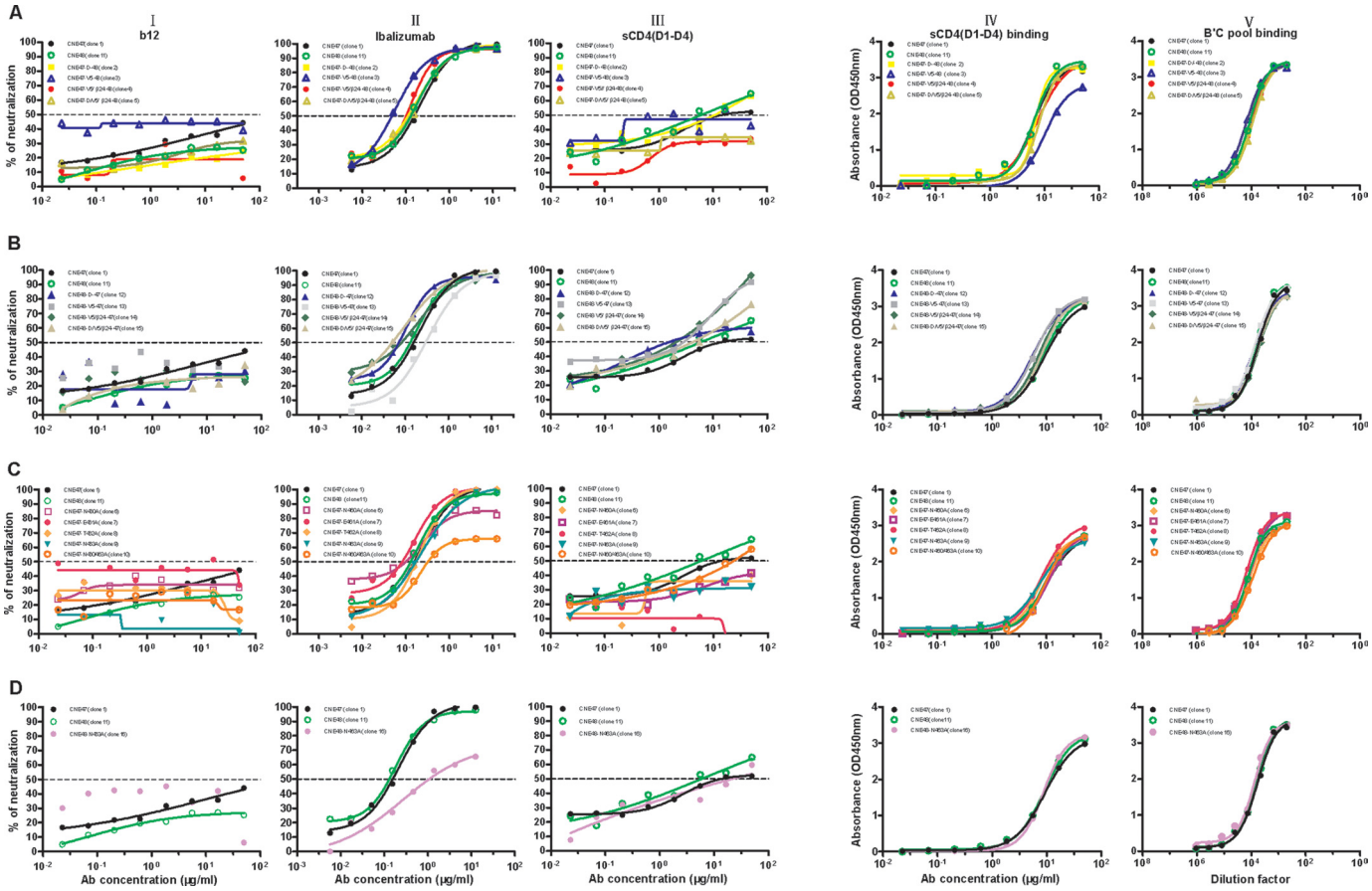

FIGURE 4. **Comparisons of CNE47- and CNE48-derived mutant viruses in terms of their neutralization sensitivities to b12, sCD4, and ibalizumab and their binding affinities with sCD4 and the HIV-1 B′C plasma pool.** None of these mutations altered b12 neutralization sensitivity or binding affinity with either sCD4 or the HIV-1 B′C plasma pool compared with parent wild-type (*columns I, IV,* and *V*). Pseudoviruses CNE48-N463A and CNE47-N460A/N463A, in which the PNGS at position 460 and/or 463 was eliminated, showed increased resistance to ibalizumab (*C* and *D*, and *column II*). All of the mutant CNE47 pseudoviruses became more resistant to sCD4 neutralization (*A*, *column III*) while those CNE48 mutants remained largely unchanged (*B*, *column III*), although sCD4 binding profiles were unchanged (*A*, *B*, *column IV*).

or binding affinity profiles in the presence of either b12 or ibalizumab, except for CNE47-N460/N463 (clone 10) and CNE48-N463 (clone 16) alanine mutant that showed significantly increased resistance to ibalizumab (Fig. 4*D*, *column II*). Furthermore, in terms of maximum inhibition by ibalizumab, only about 60% of CNE47-N460/N463 (clone 10) could be suppressed *versus* ~80% of the single knock-out strain CNE47-N463 (clone 16) compared with wild-type CNE47 (Fig. 4*C*, *column II*). These results provide some additional evidence that Asn in the V5 region of both CNE47 and CNE48 plays important roles in their sensitivity to ibalizumab and are consistent with an earlier report that the PNGS in the V5 region is critical for ibalizumab neutralization activity (30, 31).

In terms of sCD4 inhibition, almost all of the CNE47 chimeric and alanine mutants (clones 3–9), the CNE48 alanine mutant (clone 16), and the CNE30 chimeric V5 mutant (clone 23–26) showed increased resistance to sCD4, whereas no change was observed for any other mutant compared with its wild type (Table 1 and Fig. 4, *column III*). It is possible that the combination of the CNE48 V5 region in a CNE47 background or CNE23 V5 in a CNE30 background generated a chimeric CD4-binding domain that was less accessible to sCD4. However, the reverse process, inserting the V5 region of CNE47 into the CNE48 background or of CNE30 into the CNE23 background, had a small impact on the sCD4 neutralization. Furthermore, these changes were not reflected in the binding profiles of monomeric gp120 with either sCD4 or polyclonal antibodies in the B′C plasma pool (Fig. 4, *columns IV* and *V*). As a whole, these observations support the hypothesis that genetic substitutions within the V5 region not only affect pseudoviral sensitivity to VRC01 but also the overall structure of the CD4bs, altering sensitivity to sCD4 neutralization as well.

Structural Analysis Highlights the Role of Asn-460 in Interfering with the Access of VRC01 to gp120—The crystal structure of VRC01 in complex with gp120 monomer (Protein Data Bank code 3NGB) provides an excellent platform with which to study the structural basis for natural VRC01 resistance. To this end, we used the Rosetta program to model the V5 regions of both CNE47 and CNE48, generating an ensemble of 10 models for each strain. These were then docked onto VRC01 using the VRC01-gp120 crystal structure as a template (Fig. 5). Shown in the expanded *right panels* of Fig. 5, the Asn-460 residue in the V5 region of CNE47 sterically interferes with the Arg-61 residue in the CDR H2 region of VRC01. In the previously reported VRC01-gp120 structure, Arg-61 penetrates the cavity formed by the V5 region and β24-strands of gp120 (26). The presence of Asn-460 would be expected to narrow the cavity, making Arg-61 less accessible to regions of gp120 critical for VRC01

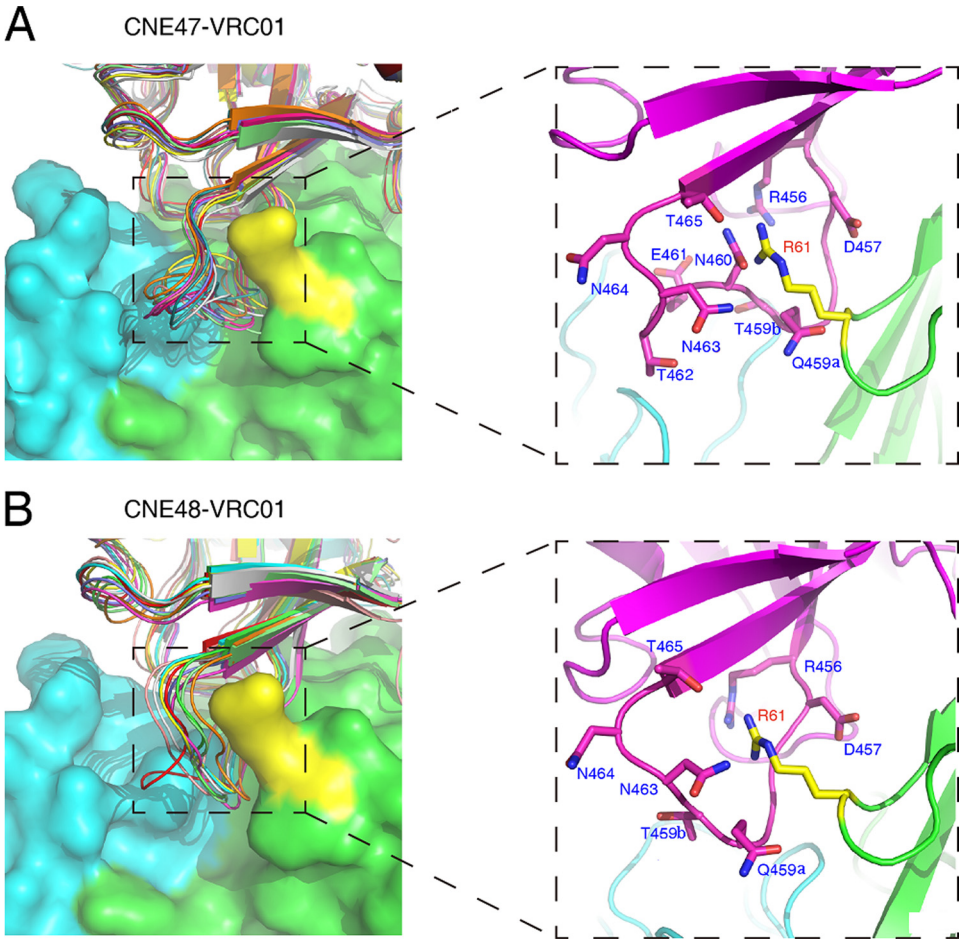

FIGURE 5. **Docking of CNE47 (*A*) and CNE48 (*B*) onto VRC01, focusing on the interaction between the V5 region of gp120 and VRC01.** An ensemble of 10 V5-modeled CNE47 and CNE48 were docked onto VRC01, as based on the reported crystal structure of VRC01 with gp120 monomer (26). The heavy chain and light chain of VRC01 are shown on the surface with *green* and *cyan* colors, respectively. The Arg-61 residue on the heavy chain of VRC01 that plays significant roles in binding is colored in *yellow*. The expanded panels display close-up views of the interaction between VRC01 Arg-61 and the surrounding residues of the gp120 V5 region.

binding. Glycosylation of Asn-460 would further block the cavity, increasing resistance to VRC01.

DISCUSSION

In this study, we identified a CRF08_BC-infected patient harboring two genetically related HIV-1 strains (CNE47 and CNE48) that displayed distinct neutralizing sensitivities to VRC01. As these clones share high levels of genetic similarity compared with those from different infected patients, these viruses offer a unique opportunity to investigate the key regions and residues that confer VRC01 resistance. Our work shows that changes in the V5 region are critical for VRC01 sensitivity between these genetically related strains. Mutagenesis analysis revealed that Asn-460, a PNGS in this region, is the major determinant of heightened resistance and weakened binding affinity with VRC01. Similar findings were also observed for two genetically unrelated strains (CNE23 and CNE30). Based on structural analysis, we hypothesize that steric interference from the long side chain of Asn-460 is the primary factor altering the interaction with VRC01 and that glycosylation may enhance this effect. In terms of other CD4bs antibodies, none of the mutations investigated in this study affected sensitivity to b12. However, more research is needed to determine their impact on a broader range of antibodies targeting this region, particularly those with VRC01-like neutralization activity. Furthermore, most changes to the V5 region did not affect interaction with ibalizumab, except for elimination of the single or double PNGS in the V5 region in CNE48 and CNE47, respectively. This is consistent with recent findings showing that having fewer or no PNGS sites in this region are strongly associated with heightened ibalizumab resistance (30, 31).

It should be noted that there are some limitations to generalization of these findings. First, although our study shows that the Asn-460 residue in the V5 region is a determining factor in VRC01 sensitivity in CRF08_B′C strains, we cannot exclude the possibility that other regions or residues would play an important role in the context of a different strain. In particular, when analyzed our database with clear phenotype and genotype information related to VRC01 neutralization, we found that among the 146 VRC01-sensitive strains, 103 (85%) have Asn at position 460, although among the 21 VRC01-resistant strains, 18 (71%) have Asn at position 460. Clearly, no correlation was identified between the Asn-460 *per se* and VRC01 resistance. However, it needs to be noted that removing Asn-460 could further heighten the overall sensitivity to VRC01 neutralization, as demonstrated for CNE30 in this work, suggesting its

contribution to overall VRC01 resistance varies between envelope clones. The resistance mechanism observed in our study is therefore more likely a strain-specific phenomenon rather than a universal explanation. Second, as the length of polymorphism exists in the V5 region between CNE47 and CNE48 and between CNE23 and CNE30, observed differences in VRC01 sensitivity could simply be caused by the insertion of extra residues, thereby altering the overall conformational structure and weakening VRC01 binding. For instance, we were surprised to find that differences in the V5 region increased resistance to sCD4, suggesting that conformational changes here may have created a novel binding domain that was less accessible to CD4.

Selection pressure from anti-CD4bs antibodies continues to drive the genetic and phenotypic diversity of HIV-1 strains within infected individuals (25, 27, 32–34). The identification of VRC01-resistant viruses has been reported in both acutely and chronically infected patients. Such strains are either the product of natural occurrence or are selected under VRC01-like immune pressures during infection. Although VRC01 has potent neutralization capacity against a broad range of heterologous strains of HIV-1, its coverage is not sufficient to preempt rapid viral evolution. Nearly all Env variants found in the recent plasma of the original VRC01 donor are now resistant to VRC01, and as we have shown here, a single mutation at Asn-460 allows the virus to circumvent neutralization. The level of resistance to VRC01, and to anti-CD4bs antibodies as a whole, is expected to increase as HIV-1 continues to spread and replicate under their selection pressure.

Ultimately, researchers hope to develop novel immunogens and immunization strategies that can induce potent anti-CD4bs antibodies (35–41). VRC01 remains one of the leading mAb candidates for prevention research and development, and the natural emergence of HIV-1 resistance poses uncertainty for its broader use. Nonetheless, detailed analyses of VRC01 escape mechanisms enhance our understanding of interactions between the virus and the immune system *in vivo*, so that we can better target strategies to address resistance. More studies are needed to fully understand how the virus circumvents neutralization; in particular, analyses of a broader range of viral strains for VRC01 sensitivity and associated biological properties. Such research will undoubtedly optimize the development process and maximize the potential use of VRC01 in clinical settings.

Acknowledgments—We are grateful to Dr. John Mascola, National Institutes of Health Vaccine Research Center, for providing bnmAb VRC01 and Dr. David Ho, Aaron Diamond AIDS Research Center, for providing ibalizumab.

REFERENCES

1. Chan, D. C., Fass, D., Berger, J. M., and Kim, P. S. (1997) Core structure of gp41 from the HIV envelope glycoprotein. *Cell* **89,** 263–273
2. Weissenhorn, W., Dessen, A., Harrison, S. C., Skehel, J. J., and Wiley, D. C. (1997) Atomic structure of the ectodomain from HIV-1 gp41. *Nature* **387,** 426–430
3. Kwong, P. D., Wyatt, R., Robinson, J., Sweet, R. W., Sodroski, J., and Hendrickson, W. A. (1998) Structure of an HIV gp120 envelope glycoprotein in complex with the CD4 receptor and a neutralizing human antibody. *Nature* **393,** 648–659
4. Zhu, P., Liu, J., Bess, J., Jr., Chertova, E., Lifson, J. D., Grisé, H., Ofek, G. A., Taylor, K. A., and Roux, K. H. (2006) Distribution and three-dimensional structure of AIDS virus envelope spikes. *Nature* **441,** 847–852
5. Dalgleish, A. G., Beverley, P. C., Clapham, P. R., Crawford, D. H., Greaves, M. F., and Weiss, R. A. (1984) The CD4 (T4) antigen is an essential component of the receptor for the AIDS retrovirus. *Nature* **312,** 763–767
6. Klatzmann, D., Champagne, E., Chamaret, S., Gruest, J., Guetard, D., Hercend, T., Gluckman, J. C., and Montagnier, L. (1984) T-lymphocyte T4 molecule behaves as the receptor for human retrovirus LAV. *Nature* **312,** 767–768
7. Alkhatib, G., Combadiere, C., Broder, C. C., Feng, Y., Kennedy, P. E., Murphy, P. M., and Berger, E. A. (1996) CC CKR5. A RANTES, MIP-1α, MIP-1βa receptor as a fusion cofactor for macrophage-tropic HIV-1. *Science* **272,** 1955–1958
8. Deng, H., Liu, R., Ellmeier, W., Choe, S., Unutmaz, D., Burkhart, M., Di Marzio, P., Marmon, S., Sutton, R. E., Hill, C. M., Davis, C. B., Peiper, S. C., Schall, T. J., Littman, D. R., and Landau, N. R. (1996) Identification of a major co-receptor for primary isolates of HIV-1. *Nature* **381,** 661–666
9. Dragic, T., Litwin, V., Allaway, G. P., Martin, S. R., Huang, Y., Nagashima, K. A., Cayanan, C., Maddon, P. J., Koup, R. A., Moore, J. P., and Paxton, W. A. (1996) HIV-1 entry into $CD4^+$ cells is mediated by the chemokine receptor CC-CKR-5. *Nature* **381,** 667–673
10. Feng, Y., Broder, C. C., Kennedy, P. E., and Berger, E. A. (1996) HIV-1 entry cofactor. Functional cDNA cloning of a seven-transmembrane, G protein-coupled receptor. *Science* **272,** 872–877
11. Zhang, L., Huang, Y., He, T., Cao, Y., and Ho, D. D. (1996) HIV-1 subtype and second-receptor use. *Nature* **383,** 768
12. Scheid, J. F., Mouquet, H., Feldhahn, N., Seaman, M. S., Velinzon, K., Pietzsch, J., Ott, R. G., Anthony, R. M., Zebroski, H., Hurley, A., Phogat, A., Chakrabarti, B., Li, Y., Connors, M., Pereyra, F., Walker, B. D., Wardemann, H., Ho, D., Wyatt, R. T., Mascola, J. R., Ravetch, J. V., and Nussenzweig, M. C. (2009) Broad diversity of neutralizing antibodies isolated from memory B cells in HIV-infected individuals. *Nature* **458,** 636–640
13. Wu, X., Yang, Z. Y., Li, Y., Hogerkorp, C. M., Schief, W. R., Seaman, M. S., Zhou, T., Schmidt, S. D., Wu, L., Xu, L., Longo, N. S., McKee, K., O'Dell, S., Louder, M. K., Wycuff, D. L., Feng, Y., Nason, M., Doria-Rose, N., Connors, M., Kwong, P. D., Roederer, M., Wyatt, R. T., Nabel, G. J., and Mascola, J. R. (2010) Rational design of envelope identifies broadly neutralizing human monoclonal antibodies to HIV-1. *Science* **329,** 856–861
14. Diskin, R., Scheid, J. F., Marcovecchio, P. M., West, A. P., Jr., Klein, F., Gao, H., Gnanapragasam, P. N., Abadir, A., Seaman, M. S., Nussenzweig, M. C., and Bjorkman, P. J. (2011) Increasing the potency and breadth of an HIV antibody by using structure-based rational design. *Science* **334,** 1289–1293
15. Scheid, J. F., Mouquet, H., Ueberheide, B., Diskin, R., Klein, F., Oliveira, T. Y., Pietzsch, J., Fenyo, D., Abadir, A., Velinzon, K., Hurley, A., Myung, S., Boulad, F., Poignard, P., Burton, D. R., Pereyra, F., Ho, D. D., Walker, B. D., Seaman, M. S., Bjorkman, P. J., Chait, B. T., and Nussenzweig, M. C. (2011) Sequence and structural convergence of broad and potent HIV antibodies that mimic CD4 binding. *Science* **333,** 1633–1637
16. Walker, L. M., Huber, M., Doores, K. J., Falkowska, E., Pejchal, R., Julien, J. P., Wang, S. K., Ramos, A., Chan-Hui, P. Y., Moyle, M., Mitcham, J. L., Hammond, P. W., Olsen, O. A., Phung, P., Fling, S., Wong, C. H., Phogat, S., Wrin, T., Simek, M. D., Protocol G Principal Investigators, Koff, W. C., Wilson, I. A., Burton, D. R., and Poignard, P. (2011) Broad neutralization coverage of HIV by multiple highly potent antibodies. *Nature* **477,** 466–470
17. Walker, L. M., Phogat, S. K., Chan-Hui, P. Y., Wagner, D., Phung, P., Goss, J. L., Wrin, T., Simek, M. D., Fling, S., Mitcham, J. L., Lehrman, J. K., Priddy, F. H., Olsen, O. A., Frey, S. M., Hammond, P. W., Protocol G Principal Investigators, Kaminsky, S., Zamb, T., Moyle, M., Koff, W. C., Poignard, P., and Burton, D. R. (2009) Broad and potent neutralizing antibodies from an African donor reveal a new HIV-1 vaccine target. *Science* **326,** 285–289
18. Barbas, C. F., 3rd, Crowe, J. E., Jr., Cababa, D., Jones, T. M., Zebedee, S. L., Murphy, B. R., Chanock, R. M., and Burton, D. R. (1992) Human monoclonal Fab fragments derived from a combinatorial library bind to respiratory syncytial virus F glycoprotein and neutralize infectivity. *Proc. Natl.*

Acad. Sci. U.S.A. **89,** 10164–10168
19. Corti, D., Langedijk, J. P., Hinz, A., Seaman, M. S., Vanzetta, F., Fernandez-Rodriguez, B. M., Silacci, C., Pinna, D., Jarrossay, D., Balla-Jhagjhoorsingh, S., Willems, B., Zekveld, M. J., Dreja, H., O'Sullivan, E., Pade, C., Orkin, C., Jeffs, S. A., Montefiori, D. C., Davis, D., Weissenhorn, W., McKnight, A., Heeney, J. L., Sallusto, F., Sattentau, Q. J., Weiss, R. A., and Lanzavecchia, A. (2010) Analysis of memory B cell responses and isolation of novel monoclonal antibodies with neutralizing breadth from HIV-1-infected individuals. *PLoS ONE* **5,** e8805
20. Wu, X., Zhou, T., Zhu, J., Zhang, B., Georgiev, I., Wang, C., Chen, X., Longo, N. S., Louder, M., McKee, K., O'Dell, S., Perfetto, S., Schmidt, S. D., Shi, W., Wu, L., Yang, Y., Yang, Z. Y., Yang, Z., Zhang, Z., Bonsignori, M., Crump, J. A., Kapiga, S. H., Sam, N. E., Haynes, B. F., Simek, M., Burton, D. R., Koff, W. C., Doria-Rose, N. A., Connors, M., NISC Comparative Sequencing Program, Mullikin, J. C., Nabel, G. J., Roederer, M., Shapiro, L., Kwong, P. D., and Mascola, J. R. (2011) Focused evolution of HIV-1 neutralizing antibodies revealed by structures and deep sequencing. *Science* **333,** 1593–1602
21. West, A. P., Jr., Diskin, R., Nussenzweig, M. C., and Bjorkman, P. J. (2012) Structural basis for germ line gene usage of a potent class of antibodies targeting the CD4-binding site of HIV-1 gp120. *Proc. Natl. Acad. Sci. U.S.A.* **109,** E2083–2090
22. Falkowska, E., Ramos, A., Feng, Y., Zhou, T., Moquin, S., Walker, L. M., Wu, X., Seaman, M. S., Wrin, T., Kwong, P. D., Wyatt, R. T., Mascola, J. R., Poignard, P., and Burton, D. R. (2012) PGV04, an HIV-1 gp120 CD4-binding site antibody, is broad and potent in neutralization but does not induce conformational changes characteristic of CD4. *J. Virol.* **86,** 4394–4403
23. Walker, L. M., Simek, M. D., Priddy, F., Gach, J. S., Wagner, D., Zwick, M. B., Phogat, S. K., Poignard, P., and Burton, D. R. (2010) *PLoS Pathog.* **68**, e1001028
24. Wu, X., Zhou, T., O'Dell, S., Wyatt, R. T., Kwong, P. D., and Mascola, J. R. (2009) Mechanism of human immunodeficiency virus type 1 resistance to monoclonal antibody B12 that effectively targets the site of CD4 attachment. *J. Virol.* **83,** 10892–10907
25. Wu, X., Wang, C., O'Dell, S., Li, Y., Keele, B. F., Yang, Z., Imamichi, H., Doria-Rose, N., Hoxie, J. A., Connors, M., Shaw, G. M., Wyatt, R. T., and Mascola, J. R. (2012) Selection pressure on HIV-1 envelope by broadly neutralizing antibodies to the conserved CD4-binding site. *J. Virol.* **86,** 5844–5856
26. Zhou, T., Georgiev, I., Wu, X., Yang, Z. Y., Dai, K., Finzi, A., Kwon, Y. D., Scheid, J. F., Shi, W., Xu, L., Yang, Y., Zhu, J., Nussenzweig, M. C., Sodroski, J., Shapiro, L., Nabel, G. J., Mascola, J. R., and Kwong, P. D. (2010) Structural basis for broad and potent neutralization of HIV-1 by antibody VRC01. *Science* **329,** 811–817
27. Li, Y., O'Dell, S., Walker, L. M., Wu, X., Guenaga, J., Feng, Y., Schmidt, S. D., McKee, K., Louder, M. K., Ledgerwood, J. E., Graham, B. S., Haynes, B. F., Burton, D. R., Wyatt, R. T., and Mascola, J. R. (2011) Mechanism of neutralization by the broadly neutralizing HIV-1 monoclonal antibody VRC01. *J. Virol.* **85,** 8954–8967
28. Shang, H., Han, X., Shi, X., Zuo, T., Goldin, M., Chen, D., Han, B., Sun, W., Wu, H., Wang, X., and Zhang, L. (2011) Genetic and neutralization sensitivity of diverse HIV-1 env clones from chronically infected patients in China. *J. Biol. Chem.* **286,** 14531–14541
29. Wang, C., Bradley, P., and Baker, D. (2007) Protein-protein docking with backbone flexibility. *J. Mol. Biol.* **373,** 503–519
30. Song, R., Franco, D., Kao, C. Y., Yu, F., Huang, Y., and Ho, D. D. (2010) Epitope mapping of ibalizumab, a humanized anti-CD4 monoclonal antibody with anti-HIV-1 activity in infected patients. *J. Virol.* **84,** 6935–6942
31. Toma, J., Weinheimer, S. P., Stawiski, E., Whitcomb, J. M., Lewis, S. T., Petropoulos, C. J., and Huang, W. (2011) Loss of asparagine-linked glycosylation sites in variable region 5 of human immunodeficiency virus type 1 envelope is associated with resistance to CD4 antibody ibalizumab. *J. Virol.* **85,** 3872–3880
32. Lynch, R. M., Tran, L., Louder, M. K., Schmidt, S. D., Cohen, M., CHAVI 001 Clinical Team Members, Dersimonian, R., Euler, Z., Gray, E. S., Abdool Karim, S., Kirchherr, J., Montefiori, D. C., Sibeko, S., Soderberg, K., Tomaras, G., Yang, Z. Y., Nabel, G. J., Schuitemaker, H., Morris, L., Haynes, B. F., and Mascola, J. R. (2012) The development of CD4-binding site antibodies during HIV-1 infection. *J. Virol.* **86,** 7588–7595
33. Pantophlet, R., Ollmann Saphire, E., Poignard, P., Parren, P. W., Wilson, I. A., and Burton, D. R. (2003) Fine mapping of the interaction of neutralizing and non-neutralizing monoclonal antibodies with the CD4-binding site of human immunodeficiency virus type 1 gp120. *J. Virol.* **77,** 642–658
34. Visciano, M. L., Tuen, M., Gorny, M. K., and Hioe, C. E. (2008) *In vivo* alteration of humoral responses to HIV-1 envelope glycoprotein gp120 by antibodies to the CD4-binding site of gp120. *Virology* **372,** 409–420
35. Dey, B., Pancera, M., Svehla, K., Shu, Y., Xiang, S. H., Vainshtein, J., Li, Y., Sodroski, J., Kwong, P. D., Mascola, J. R., and Wyatt, R. (2007) Characterization of human immunodeficiency virus type 1 monomeric and trimeric gp120 glycoproteins stabilized in the CD4-bound state. Antigenicity, biophysics, and immunogenicity. *J. Virol.* **81,** 5579–5593
36. Douagi, I., Forsell, M. N., Sundling, C., O'Dell, S., Feng, Y., Dosenovic, P., Li, Y., Seder, R., Loré, K., Mascola, J. R., Wyatt, R. T., and Karlsson Hedestam, G. B. (2010) Influence of novel CD4 binding-defective HIV-1 envelope glycoprotein immunogens on neutralizing antibody and T-cell responses in nonhuman primates. *J. Virol.* **84,** 1683–1695
37. Feng, Y., McKee, K., Tran, K., O'Dell, S., Schmidt, S. D., Phogat, A., Forsell, M. N., Karlsson Hedestam, G. B., Mascola, J. R., and Wyatt, R. T. (2012) Biochemically defined HIV-1 envelope glycoprotein variant immunogens display differential binding and neutralizing specificities to the CD4-binding site. *J. Biol. Chem.* **287,** 5673–5686
38. Koch, M., Pancera, M., Kwong, P. D., Kolchinsky, P., Grundner, C., Wang, L., Hendrickson, W. A., Sodroski, J., and Wyatt, R. (2003) Structure-based, targeted deglycosylation of HIV-1 gp120 and effects on neutralization sensitivity and antibody recognition. *Virology* **313,** 387–400
39. Li, Y., Svehla, K., Mathy, N. L., Voss, G., Mascola, J. R., and Wyatt, R. (2006) Characterization of antibody responses elicited by human immunodeficiency virus type 1 primary isolate trimeric and monomeric envelope glycoproteins in selected adjuvants. *J. Virol.* **80,** 1414–1426
40. Pancera, M., Lebowitz, J., Schön, A., Zhu, P., Freire, E., Kwong, P. D., Roux, K. H., Sodroski, J., and Wyatt, R. (2005) Soluble mimetics of human immunodeficiency virus type 1 viral spikes produced by replacement of the native trimerization domain with a heterologous trimerization motif. Characterization and ligand binding analysis. *J. Virol.* **79,** 9954–9969
41. Saha, P., Bhattacharyya, S., Kesavardhana, S., Miranda, E. R., Ali, P. S., Sharma, D., and Varadarajan, R. (2012) Designed cyclic permutants of HIV-1 gp120. Implications for envelope trimer structure and immunogen design. *Biochemistry* **51,** 1836–1847